EFFECTS OF A TRANSVERSE MAGNETIC FIELD ON TURBULENT-NATURAL CONVECTION FLUID FLOW IN A CUBICAL ENCLOSURE

J. K. Kwanza, P. K. Ndung'u, and M. Kinyanjui
Department of Pure and Applied Mathematics Department, Jomo Kenyatta University of Agriculture and Technology, Nairobi
E-mail: kwanzakioko@yahoo.com

ABSTRACT

A numerical simulation is used to study turbulent natural convection flow in a cubical cavity whereby a transverse magnetic field is applied along the vertical axis. The cavity is heated steadily on the lower horizontal surface and cooled on the top opposite side. The fluid is passed on from an inlet and exit on the opposite vertical side. The fluid in question is incompressible, electrically conducting and the fluid flow is unsteady. The standard $k-\varepsilon$ model is used to model the mean flow equations of heat flux and momentum flux and is approximated by Boussinesq approximation and the generalised gradient diffusion hypothesis. Effects of the magnetic field on velocity, temperature and heat transfer of the fluid inside the cavity are investigated. The Reynolds averaging of Navier-Stokes equations method is used to decompose the equations and match them through time and space. The finite difference method is used to arrive at the results. Effects of various parameters on velocity, temperature and the rate of heat transfer are analysed with the help of graphs and tables. It is found that magnetic field suppresses turbulence for an electrically conducting fluid flow.

Key words: Natural convection, turbulent flow, transverse magnetic field, heat transfer, finite difference method

NOMENCLATURE

Symbol	Quantity
A_{inlet}, A_{outlet}	Outlet and inlet area, m^2
C_p	Specific heat at constant pressure, $\frac{KJ}{Kg \cdot K}$
$C_\mu, C_{\varepsilon 1}, C_{\varepsilon 2}, C_{\varepsilon 3}, C_{\varepsilon k}$	Empirical *k-e* model constants
e	Kinetic energy, J
E	Total energy
g_i	Gravitational acceleration in tensor notation , m/s^2
Gr	Grashof number
Gn	Gravity number
Ha	Hartmann number
H_0	Magnetic field intensity, Wb/m^2
I	Turbulent intensity at the outlet and inlet, m^2/s
k	Turbulent energy, J
Nu	Nusselt number
Pr	Prandtl number
Re	Reynolds number
Ra	Rayleigh number
S	Entropy, $\frac{J}{Kg \cdot K}$
T_h	Temperature on the hot wall, **K**
T_c	Temperature at the cold wall, **K**
T_0	Reference temperature, **K**
T	Temperature, **K**
t	Time, s
u, v, w	Velocity components, m/s
U_t	Tangential velocity component, m/s
$U_{inlet/jet}$	Velocity at the inlet and outlet, m/s
U_i, U_j, U_k	Tensor notation for velocity, m/s
$\tilde{U}$	Time advanced velocity values, s
$U_{i,j,k}$, $V_{i,j,k}$, $W_{i,j,k}$	Velocities at the cell, m/s
V	Characteristic velocity, m/s
$V_{outlet/jet}$	Velocity at the inlet and outlet, m/s
x_j	Direction tensor notation, m
y_n	Normal distance to the inlet and outlet, m

Δt	Time step, s
$\Delta x, \Delta y, \Delta z$	Cell dimensions, m

Greek Symbols

ρ	Density, kg m^{-3}
σ	Electrical conductivity, Ω^{-1} / m
μ	First coefficient of viscosity, kg/m.s
μ_s	Second coefficient of viscosity, kg/m.s
μ_e	Magnetic permeability
μ_t	Eddy-viscosity, m^2/s
δ_{ij}	Kronecker delta
τ_{ij}	Viscous stress tensor notation
λ	Thermal conductivity, W/m K
α	Thermal diffusivity, m^2/s
$\dot{\alpha}$	Donor cell coefficient
ν	Kinematic viscosity, m^2/s
$\sigma_k, \sigma_\varepsilon, \sigma_T$	Constants in the k-e model
ν, ν_t	Fluid viscosity, turbulent viscosity, m^2/s
β	Thermal coefficient, K^{-1}
ε	Turbulence dissipation rate, m^2/s^3
τ	Turbulent time scale, s
Γ_i	Tensor notation for a function in turbulent equation
Π	Function in turbulent equation
Θ	Nondimensional temperature
θ	Function in turbulent equation, **K**
ξ	Relaxation factor

Abbreviations

FDM	Finite difference Method
MAC	Marker and Cell Representation
MHD	Magneto hydrodynamics
FUX, FUY, FUZ	Convective terms in momentum equation
FKX, FKY, FKZ	Convective terms in the turbulent kinetic energy equation

FEX, FEY, FEZ,	Convective terms in the turbulent energy rate of dissipation equation.
DFFR	Desired fluid flow rate, m/s
BDF	Boundary differential finite method
GGDH	Generalised diffusion hypothesis

1.0 INTRODUCTION

Turbulent natural convection is observed in many circumstances such as in passive solar rooms, equalisation of temperature in large nuclear reactor containment filled with a conducting fluid and for removal of the heat generated within a casing of electronic equipment by integrated circuits. Generally the study is also applicable to systems involving high temperature plasmas applicable to liquid-metal and magneto-fluid dynamic power generation systems.

The study of MHD's started in the early 1830's with Faraday (1839) where he experimented on passing of an electrically conducting fluid between poles of a magnet in a vacuum glass. Since then a lot of research in this area has been done. Hoogendorn (1986) investigated the effects of various parameters on natural convection in an enclosure, the skin friction and the shear stress on the boundary layer. Alboussiere *et al* (1992) analysed the effects of a transverse magnetic field in a rectangular enclosure, where effects of various parameters on temperature and velocity profiles were analysed. Effects of various parameters were also studied towards heat distribution in the enclosure. Alboussiere *et al* (1993) later studied the effect of slight non-uniformity of the magnetic field on MHD natural convection and established effects of the magnetic field on heat transfer in an enclosure. Branover *et al* (1993) studied the effects of a transverse magnetic field on the intensity profiles of turbulent velocity distribution in a rectangular cross-section. Henry and Kaddeche (1993) studied the stability of methods used in solving the turbulent natural convection problems. Stabilisation laws of buoyant flows under a weak magnetic field were presented. Hague and Arajs (1994) undertook both numerical and experimental studies on convective heat transfer for different kinds of fluids namely, kerosene, silicon oil and nitrogen in an enclosure. They analyzed the effects of magnetic, electric and electromagnetic forces on heat transfer. Aleksandrova and Molokov (2000) studied a three-dimensional buoyant convection in a rectangular cavity with differentially heated walls in a strong magnetic field and analysed the effects of varying the magnetic field on fluid flow. Ming and Tang (2001) used several known time stepping approaches including the second-order boundary differential finite method (BDF) inclusive of the 4^{th}-order BDF together with the Crank-Nicholson method on a cavity problem to study the velocity and temperature distributions in a square cavity.

The studies above did not analyse the effects of magnetic field to velocity, temperature distribution and rate of heat transfer in a cubical enclosure having an outlet and inlet on opposite sides despite most being concerned about natural convection with use of different fluids in enclosures which is our present study.

2.0 MATHEMATICAL ANALYSIS

We consider a turbulent natural convection fluid flow of a heat and electrically conducting viscous incompressible fluid inside a differentially heated cubical enclosure with a transverse uniform magnetic field of strength H_0 applied on its vertical axis. The cavity is heated on the lower horizontal surface (T_h) and cooled on the top surface (T_c). The fluid flows inside the enclosure from an inlet and exits' on the opposite side is taken to have Prandtl number of 0.71, which corresponds to air. We consider some physical characteristics of the fluid to be constant like: dynamic viscosity ν, thermal conductivity λ, and specific heat rate on the constant pressure for averaged temperature T_0. All temperatures are of low intensity and therefore we can neglect radiation. Density is considered as constant value but for buoyant term it's linearised by the relation: $\rho(T) = \rho(T_0) - \beta\rho(T_0)(T - T_0)$.

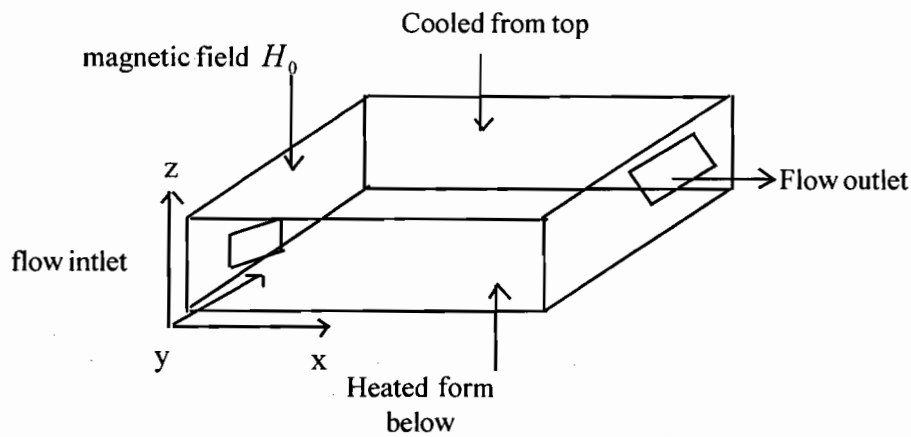

Figure 1: The geometry of the problem and flow configuration with the coordinate system

Both the fluid and the cavity walls are initially in thermal equilibrium, having a temperature T_0. Two of the cavity walls (horizontal) are isothermal whereas the four vertical walls are adiabatic (thermally insulated). The cold wall is kept at the initial temperature ($T_c = T_0$) and the temperature of the hot wall is suddenly increased at time t = 0 to . Thereafter at t > 0 the 'hot' isothermal wall temperature is maintained at T_h. The cold wall temperature is maintained at T_c.

Due to the temperature gradient applied between the two walls, the fluid inside the cavity initially at rest begins to move. The buoyancy forces act to accelerate the fluid creating a horizontal viscous layer with large velocities transporting the fluid to the top of the cavity. The type of flow occurring is determined by the relative values of the dimensionless parameters; Rayleigh and Prandtl numbers.

2.1 Turbulence Model

The governing equations based on the standard model of Piomelli (1999) for turbulent natural convection problems are

$$\frac{\partial U_i}{\partial x_j} = 0 \quad \text{.....(1)}$$

$$\frac{\partial U_i}{\partial t'} + \frac{\partial}{\partial x_j'}\left(U_i U_j\right) = (Ra) g_i \rho \beta \left(T - T_0\right)_i - (Ha)\frac{\sigma \mu_e^2 H_0^2 U_i}{\rho} + (\mathrm{Pr})\frac{\partial}{\partial x_j'}\left\{\mu \frac{\partial U}{\partial x_j'}\right\} + \frac{\partial}{\partial x_j'}\left\{-\rho u_i u_j\right\} \quad \text{.....(2)}$$

$$\frac{\partial}{\partial t}\left(c_p \rho \Theta + c_p \overline{\rho \Theta}\right) + \frac{\partial}{\partial x_j}\left(c_p \rho U_j \Theta\right) = \left(\frac{1}{\mathrm{Re.Pr}}\right)\frac{\partial \Theta}{\partial x_j} + \frac{\partial}{\partial x_j}\left(\lambda \frac{\partial \Theta}{\partial x_j} - c_p \rho u_i \Theta - c_p \rho u_j \Theta\right) + (Gn)\left(\tau_{ij}\frac{\partial U_k}{\partial x_k} - \mu\left(\frac{\partial u_i}{\partial x_j} + \frac{\partial u_j}{\partial x_i}\right)\frac{\partial u_i}{\partial x_j}\right) \quad \text{.....(3)}$$

$$\frac{\partial \rho k}{\partial t} + \frac{\partial}{\partial x_j}\left(\rho U_j k\right) = -(Ra) g_i \beta \frac{k}{\varepsilon} u_i u_j \frac{\partial \Theta}{\partial x_j} + (Ha)\sigma \mu_e^2 H_0^2 U_i - (\mathrm{Pr})\left(\mu\left(\frac{\partial u_i}{\partial x_j} + \frac{\partial u_j}{\partial x_i}\right)\frac{4}{3}\left(\mu \frac{\partial U_k}{\partial x_k}\right) + \frac{\partial}{\partial x_j}\left((\mu + \frac{\mu_t}{\sigma_k})\frac{\partial k}{\partial x_j}\right) - \mu\left(\frac{\partial U_i}{\partial x_j}\right)^2\right) \quad \text{.....(4)}$$

$$\frac{\partial}{\partial t}(\rho\varepsilon)+\frac{\partial}{\partial x_j}(\rho U_j\varepsilon)=\begin{Bmatrix} 2C_{\varepsilon 1}\left(-\rho u_i u_j\frac{\partial U_i}{\partial x_j}\right)-(Ra)g_i\beta C_0\frac{k}{\varepsilon}u_i u_j\frac{\partial\Theta}{\partial x_j} \\ -(Ha\,\mathrm{Re})\sigma\mu_e^2H_0^2U_i \\ +(\mathrm{Pr})\left(\rho C_{\varepsilon 4}k\frac{\partial U_k}{\partial x_k}\right)-(\mathrm{Pr})C_{\varepsilon 2}\varepsilon \end{Bmatrix}\frac{\varepsilon}{k}\frac{\partial}{\partial x_j}\left(\frac{\mu}{\sigma_k}\frac{\partial\varepsilon}{\partial x_j}\right) \quad \text{.....(5)}$$

Where $\mathrm{Re}=\frac{\rho UL}{\mu}$,

$Ra=\frac{g\beta\Delta TL^3}{\rho U^2}, \mathrm{Pr}=\frac{\mu C_p}{k}, Ha=\frac{\sigma\mu_e^2H_o^2\upsilon}{\rho U^2}, \theta=\frac{T-T_c}{T_h-T_c}, Gn=\frac{\mu U}{C_p\rho\Delta TL}$ and

L,T,U , and L,T,U are the reference length, Temperature and Velocity respectively.

$$\overline{\tau_{ij}}=\mu\left(\frac{\partial\overline{U_i}}{\partial x_j}+\frac{\partial\overline{U_j}}{\partial x_i}\right)+\mu_s\delta_{ij}\frac{\partial\overline{U_k}}{\partial x_k} \text{ and } \overline{\Phi}=\overline{\tau_{ij}}\frac{\partial\overline{u_i}}{\partial x_j}+\overline{\tau_{ij}\frac{\partial u_i'}{\partial x_j}} \quad \text{.....(6)}$$

The model constants are

$C_\mu=0.09, C_{\varepsilon 1}=1.44, C_{\varepsilon 2}=1.92, C_{\varepsilon 3}=0.8, C_{\varepsilon 4}=0.33, \sigma_k=1.0, \sigma_\varepsilon=1.3\ and\ \sigma_T=0.9$

(7)

Due to the presence of extra terms in the turbulent kinetic energy and rate of dissipation equations (equations 4 and 5) we modelled the turbulent momentum and turbulent heat flux as by commonly used generalised gradient diffusion hypothesis (GGDH) of Daly and Harlow (1970) which was used by Ince and Launder (1985) to account for the interaction between shear stress and span wise temperature gradient. That is,

$$\overline{u_iT}=-C_{\varepsilon 1}u_iu_j\frac{\varepsilon}{k}\frac{\partial T}{\partial x_k} \text{ and } \overline{u_iu_j}=-\nu_t\left\{\frac{\partial U_i}{\partial x_j}+\frac{\partial U_j}{\partial x_i}\right\}+\frac{2}{3}k\delta_{ij}$$

where $\nu_t=C_\mu\frac{k^2}{\varepsilon}, \quad C_\mu=0.09$ .....(8)

The boundary and initial conditions pertaining to the study are:

Table 1: Summary of boundary and initial conditions pertaining the study

Boundary conditions	*Velocities*	*Temperature*	*Turbulence Energy*	*Turbulence Dissipation*
Inlet	$U_t = 0$ $U_n = U_{jet}$	T_{inlet}	$k_{inlet} = \frac{3}{2} I_u^2 U_{jet}^2$	$\varepsilon_{inlet} = \frac{k_{inlet}^{\frac{3}{2}}}{\lambda H}$
Outlet	$U_t = 0$ $U_{outlet} = U_{jet} \frac{\rho A\|_{inlet}}{\rho A\|_{outlet}}$	$\frac{\partial T}{\partial x_n} = 0$	$\frac{\partial k}{\partial x_n} = 0$	$\frac{\partial \varepsilon}{\partial x_n} = 0$
WallsNon-slip	$U_t = 0$ $U_n = 0$	$\frac{\partial T}{\partial x_n} = \frac{h}{k}(T_h - T_c)$	-	-
Near the Walls	$U_n = 0$ $\left.\frac{\partial U_t}{\partial x_n}\right\|_{walls} = \frac{m U_t}{y_n}$	$\frac{\partial T}{\partial x_n} = \frac{h}{k}(T_h - T_c)$	$\frac{\partial k}{\partial x_n} = 0$	$\varepsilon = \frac{2vk}{y_n^2}$ $\varepsilon = \frac{\left(C_\mu^{\frac{1}{2}} k\right)^{\frac{3}{2}}}{k y_n}$

2.2 Solution of the Problem by Finite Difference Method (the Marker and Cell (Mac))

This investigation uses the MAC method of defining variables within the flow field, Harlow *et al.* (1965). The method is useful as it assumes that pressure is invariant whereby the Boussinesq approximation is comfortably applied. For a given cell the dimensions and, velocities are defined at the centre of the cell as shown in the figure below.

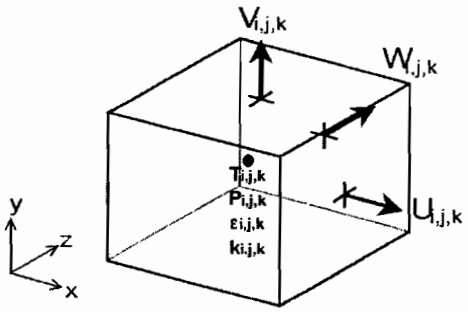

Figure 2: Marker-and-cell representation

We extend the concepts to three-dimension which incorporates the starting point of mathematical formulation of the study assuming that, density is constant: Since the mean velocity values need only be considered when imposing the scheme, the finite difference equation for continuity equation may be used to impose the conservation of mass for the turbulent flow viz;

$$\frac{1}{\Delta x}\left(U_{i,j,k}-U_{i-1,j,k}\right)+\frac{1}{\Delta y}\left(V_{i,j,k}-V_{i,j-1,k}\right)+\frac{1}{\Delta z}\left(W_{i,j,k}-W_{i,j,k-1}\right)=0 \quad \text{.....(9)}$$

For convenience and ease in implementation into a numerical scheme, the momentum equation is written using a new term Γ_i

$$\tilde{U}_{i,j,k} = U_{i,j,k} + \Delta t(\Gamma_x - FUX - FUY - FUZ) \quad \text{.....(10)}$$

Where FUX, FUY and FUZ are the convective terms where incase of x, y or z-component the terms are dropped for the rest of the cases. (~) denotes any value at time $t + \Delta t$. Awbi (1989) introduced a constant that ensures numerical stability without avoidable round-off errors. The coefficient is called the donor-cell coefficient ($\hat{\alpha}$) representing the amount of upstream differencing used in determining first derivatives.

The donor-cell coefficient is given by $\hat{\alpha} = \zeta \cdot \max\left|\frac{|U|\Delta t}{\Delta x}; \frac{|V|\Delta t}{\Delta y}; \frac{|W|\Delta t}{\Delta z}\right|$,

where ζ is a relaxation constant used in buoyant flows varying from 1.2 to 1.5. The convective terms in form of FDM are given as

$$FUX = \frac{1}{4\Delta x}\left\{\begin{array}{c}\left(U_{i,j,k} + U_{i+1,j,k}\right)^2 + \hat{\alpha}\left|U_{i,j,k} + U_{i+1,j,k}\right|\left(U_{i,j,k} - U_{i+1,j,k}\right) - \left(U_{i-1,j,k} + U_{i,j,k}\right)^2 \\ -\hat{\alpha}\left|U_{i-1,j,k} + U_{i,j,k}\right|\left(U_{i-1,j,k} - U_{i,j,k}\right)\end{array}\right\}$$

$$FUY = \frac{1}{4\Delta y}\left\{\begin{array}{c}\left(V_{i,j,k} + V_{i+1,j,k}\right)\left(U_{i,j,k} + U_{i,j+1,k}\right) + \hat{\alpha}\left|V_{i,j,k} + V_{i+1,j,k}\right|\left(U_{i,j,k} - U_{i,j+1,k}\right) - \left(V_{i,j-1,k} + V_{i+1,j-1,k}\right) \\ \left(U_{i,j-1,k} + U_{i,j,k}\right) - \hat{\alpha}\left|V_{i,j-1,k} + V_{i+1,j-1,k}\right|\left(U_{i,j-1,k} - U_{i,j,k}\right)\end{array}\right\} \quad \text{.....(11)}$$

$$FUZ = \frac{1}{4\Delta z}\left\{\begin{array}{c}\left(W_{i,j,k} + W_{i+1,j,k}\right)\left(U_{i,j,k} + U_{i,j,k+1}\right) + \hat{\alpha}\left|W_{i,j,k} + W_{i+1,j,k}\right|\left(U_{i,j,k} - U_{i.j,k+1}\right) \\ -\left(W_{i,j,k-1} + W_{i+1,j,k-1}\right)\left(U_{i,j,k-1} - U_{i,j,k}\right) - \hat{\alpha}\left|W_{i,j,k-1} + W_{i+1,j,k+1}\right|\left(U_{i,j,k+1} - U_{i,j,k}\right)\end{array}\right\}$$

The same can be done for the y and z- components.

The energy equation, Lilley (1991) can be treated as a scalar quantity together with the turbulent energy (k) and the dissipation rate (ε). Thus for any scalar quantity Φ we can obtain an explicit equation for the time-advanced scalar quantity. Hence the energy equation may be approximated by the following set of equations.

$$\tilde{T}_{i,j,k} = T_{i,j,k} + \Delta t(VIST - FTX - FTY - FTZ) \quad \text{.....(12)}$$

where

$$
\left.
\begin{aligned}
FTX &= \frac{1}{2\Delta x}\left\{\begin{aligned} &U_{i,j,k}\left(T_{i,j,k}+T_{i+1,j,k}\right)+\hat{\alpha}\left|U_{i,j,k}\right|\left(T_{i,j,k}-T_{i+1,j,k}\right)\\ &-U_{i-1,j,k}\left(T_{i-1,j,k}+T_{i,j,k}\right)-\hat{\alpha}\left|U_{i-1,j,k}\right|\left(T_{i-1,j,k}-T_{i,j,k}\right)\end{aligned}\right\}\\
FTY &= \frac{1}{2\Delta y}\left\{\begin{aligned} &V_{i,j,k}\left(T_{i,j,k}+T_{i+1,j,k}\right)+\hat{\alpha}\left|V_{i,j,k}\right|\left(T_{i,j,k}-T_{i-1,j,k}\right)\\ &-V_{i-1,j,k}\left(T_{i-1,j,k}+T_{i,j,k}\right)-\hat{\alpha}\left|V_{i-1,j,k}\right|\left(T_{i-1,j,k}-T_{i,j,k}\right)\end{aligned}\right\}\\
FTZ &= \frac{1}{2\Delta z}\left\{\begin{aligned} &W_{i,j,k}\left(T_{i,j,k}+T_{i+1,j,k}\right)+\hat{\alpha}\left|W_{i,j,k}\right|\left(T_{i,j,k}-T_{i-1,j,k}\right)\\ &-W_{i-1,j,k}\left(T_{i-1,j,k}+T_{i,j,k}\right)-\hat{\alpha}\left|W_{i-1,j,k}\right|\left(T_{i-1,j,k}-T_{i,j,k}\right)\end{aligned}\right\}\\
VIST &= \alpha\left\{\begin{aligned} &\frac{1}{\Delta x^2}\left(T_{i+1,j,k}-2T_{i,j,k}+T_{i-1,j,k}\right)+\frac{1}{2\Delta y^2}\left(T_{i,j+1,k}-2T_{i,j,k}+T_{i,j-1,k}\right)\\ &+\frac{1}{2\Delta z^2}\left(T_{i,j,k+1}-2T_{i,j,k}+T_{i,j,k-1}\right)\end{aligned}\right\}
\end{aligned}
\right\} \quad \text{.....(13)}
$$

where the value of is to be determined in the same way as one in the momentum differences. For turbulent energy (k) the equation can be written in finite differenced equations as

$$
\tilde{k}_{i,j,k} = k_{i,j,k} + \Delta t\left\{\begin{aligned} &2g_x\beta(k)^2\varepsilon^{-1}\left(T_{i,j,k}-T_0\right)+\frac{\sigma\mu_e{}^2H_0{}^2}{\rho}\left(U_{i,j,k}-U_{i-1,j,k}\right)+\nu_t\Pi\\ &+\Phi(k)-FKX-FKY-FKZ-\varepsilon\end{aligned}\right\} \quad \text{.....(14)}
$$

Since the turbulent energy (k) is a scalar quantity, the terms FKX, FKY and FKZ may be determined in the same way as the ones in equations (13). The equation of energy dissipation (5) can be written for time-advanced values as

$$
\tilde{\varepsilon}_{i,j,k} = \varepsilon_{i,j,k} + \Delta t\left\{\begin{aligned} &\Phi(\varepsilon)-2C_{\varepsilon 3}k\frac{\partial U_i}{\partial x_j}-2g_i\beta C_\upsilon\frac{k^2}{\varepsilon}\left(T_{i,j,k}-T_0\right)+\frac{\sigma\mu_t{}^2H_0^2}{\rho}\left(U_{i,j,k}-U_{i-1,j,k}\right)\frac{1}{\Delta x_i}\\ &+C_{\varepsilon 4}k\frac{1}{\Delta x_i}\left(U_{i,j,k}-U_{i-1,j,k}\right)-C_{\varepsilon 2}\varepsilon-FEX-FEY-FEZ\end{aligned}\right\} \quad \text{.....(15)}
$$

The values FEX, FEY and FEZ can be determined similarly as ones in equation (13). For numerical stability the material fluid was not allowed to move a distance greater than one cell over a given time step. This was achieved by imposing the cell transit time (CTT) hypothesis as

$$(\Delta t)_1 = \xi \cdot \min\left\{\frac{\Delta x}{|U_{\max}|}; \frac{\Delta y}{|V_{\max}|}; \frac{\Delta z}{|W_{\max}|}\right\} \text{ Where } 1.2<\xi<1.5 \quad \text{.....(16)}$$

Also for the turbulent viscosity that is considered nonzero, momentum is contained and assumed not to diffuse more than one cell at a given time step. This was achieved by

$$(\Delta t)_2 = \frac{1}{2\nu_t}\min\left((\Delta x)^2;(\Delta y)^2;(\Delta z)^2\right) \quad \text{.....(17)}$$

Similarly, the turbulent kinetic energy was controlled by

$$(\Delta t)_3 = \frac{1}{2\nu_t}\left(\frac{1}{(\Delta x)^2}+\frac{1}{(\Delta y)^2}+\frac{1}{(\Delta z)^2}\right)^{-1} \quad \text{.....(18)}$$

To determine temperature values and model buoyancy an additional criterion was imposed that heat cannot diffuse more than one cell per a time step. The criterion used was

$$(\Delta t)_4 = \frac{1}{2\alpha}\left(\frac{1}{(\Delta x)^2}+\frac{1}{(\Delta y)^2}+\frac{1}{(\Delta z)^2}\right)^{-1} \quad \text{.....(19)}$$

The uniform grid used had 81x81x81nodes and very small changes were noted with reduction of the number of nodes used.

3.0 DISCUSSION OF RESULTS

Numerical computations are performed for the velocity, temperature and rate of heat transfer inside the enclosure. Contours at different positions where a certain axis is fixed, showing the distribution of velocity magnitudes and temperature distributions in the enclosure is presented. A uniform velocity distribution is generally assumed over the inlet area. Imposing this boundary condition allows the tangential velocity to be zero ($U_t = 0$). The normal component (U_n) is then determined based on the desired fluid flow rate (DFFR) (Awbi 1990) using the equation;

$$U_{jet} = \frac{\text{DFFR x Volume of Enclosure}}{\text{3600 x area of inlet}}$$

The inlet velocity was taken as 0.175. Similarly, a uniform velocity distribution is assumed at the enclosure outlet. Tangential velocities are to be considered zero ($U_t = 0$), while the normal velocity is to be determined by the mass balance on the enclosure given by

$$U_{outlet} = U_{jet}\frac{(\rho A)_{inlet}}{(\rho A)_{oulet}}$$

The outlet velocity was taken as 2.1 .The results presented here are with Rayleigh number ranging between $5x10^{-11}$ and $5x10^{13}$, implying that the flow is turbulent. Velocity and temperature profiles are first computed in the absence of the magnetic field, Ha=0 (figures 3, 4, 5 and 6) for Reynolds number 750 and Rayleigh number $50x10^{11}$. Velocity and temperature profiles are then computed in presence of magnetic field, Ha=50(figure 7 to 20). Simulations are performed for the enclosure with fluid entering at a temperature difference between 9°K and 36°K. 36°K corresponds to the Rayleigh number $5x10^{11}$ and Pr = 0.71 corresponds to air.

3.1 Velocity Profiles

Generally, it is evident from figures 3, 5, 7, 9, 11, 13 and 15 that the cubical cavity problem has two distinct flow patterns:

(i) Growth of the boundary layer along the wall.

(ii) Recirculation motion in the core region.

Growth of boundary layer is interpreted from the velocity intensity at the layers close to both the hot and cold walls. The main recirculating flow splits into smaller counter rotating eddies at the cavity core forming roll cells. The smaller inner eddies are stretched towards the top retaining the dominance of the main circulation. With increase in the Rayleigh number, there is a change of fluid flow patterns with inner secondary eddies moving closer to the hot and cold walls

From Figure 7, it is noted that when the magnetic field is applied transversely to the direction of fluid flow, the velocity decreases. From Figure 5, it is noted that the roll cells are closer to the hot surface. Increase in Raleigh number and introduction of magnetic pushes the roll cells in the core of the cavity as can be noted from Figure 7. From Figures 9, 11 and 13, no significant change is noted from the roll cells. Velocity intensity almost doubled with increase in Rayleigh number as can be noted from Figures 7 and 9. From Figure 15, it is noted that the velocity intensity is greatest mid-way between the roll cells. This may be explained by the increase in Rayleigh number from $5x10^{11}$ to $5x10^{13}$. From this we note that in presence of a transverse magnetic field, increase in Rayleigh number leads to increase in the velocity intensity of a conducting fluid.

3.2 Temperature Profiles

Temperature differences within the cavity will obviously cause density differences throughout the enclosure, which are the cause of buoyant effects. However the maximum temperature difference is 27^0k. It is assumed that density of the fluid did not change irrespective of temperature difference within the enclosure. Figures 4 and 6 were obtained in the absence of magnetic field. It is noted that the temperature distribution in the enclosure is minimal irrespective of the fluid being heated. The profiles show less heat is transferred to the rest of the enclosure, as the profiles are closely concentrated at the base of the cavity. With introduction of magnetic field and

increase in Rayleigh number, we compare Figures 6 and 8 whereby it is noted that after these alterations, temperature distribution inside the cavity increased. Temperature at the core of the cavity increased compared to the sections near the hot surface. From Figures 8, 10, 12, 14 and 16, it is noted that on the bottom right and left corners of the cavity temperature is low compared to the rest of the cavity. This is due to the onset of a cold downdraught of cool fluid replacing heated fluid at the base. The graphical plots comparison of Figures 8 and 10 sufficiently show that there are no significant changes in temperature distribution. Both Figures were plotted at Rayleigh number 5×10^{12} and Hartmann number equal to 50. The only noticeable thing is at the core of the cavity where temperature is greater compared to the bottom left and right corners of the cavity. Comparing between Figures 6 and 8, it is noted that there is an enhanced temperature distribution after increase in Rayleigh number and introduction of magnetic field as Figure 8 was plotted after the two alterations. Increase in Rayleigh number enhances temperature distribution as can be noted from Figures 8 and 10. Figures 12 and 14 certainly highlight that as Rayleigh number increases; temperature distribution within the enclosure increases but magnetic field hinders temperature distributions within a cavity filled with an electrically conducting fluid. Increasing the Rayleigh number to 5×10^{13} as plotted in Figure 16 increased the temperature distribution and the profiles can be clearly distinguished at various positions within the cavity. Comparing the three situations where Rayleigh numbers were changed and introduction of magnetic field, we deduce that presence of magnetic field leads to a decrease in temperature gradient. To see what happens across the enclosure, velocity profiles and Temperature distributions were obtained at the locations $x = 0.5$ and $x = 0.9$ (Figures 17, 18, 19 and 20).The trends were found to be similar to those illustrated in Figures7and 8.

3.3 Rate of Heat Transfer

Knowledge of heat transfer along the hot and cold walls is valuable to thermal engineers and designers. Nusselt number represents the desired non-dimensional parameter of interest, which is the ratio of heat convected from the fluid to the wall. It is given by the relation $Nu = \pm \left.\frac{\partial \theta}{\partial x}\right|_{horizontal\ walls}$ where $x = \frac{x'}{L}$

and θ is the dimensionless temperature as defined earlier. In the expression above, the negative sign essentially implies transfer of heat from the cold wall to the fluid while the positive signifies transfer of heat to the fluid from the hot wall. The Nusselt number distribution within the cavity is plotted in Figure 21. The distribution of fluid Nusselt number is asymmetric between the hot and cold walls.

The number is greatest at the base of the cavity but reduces as the height of the cavity increases. Thus, there is more heat transfer to the fluid from the hot surface than on the cold surface. This is due to the fact that some fluid exits before it reaches

the top of the compartment. Also, the magnetic field applied transversely from the top of the cavity has greater effect on the upper fluid particles than the lower rising fluid particles. This impedes heat transfer to the uppermost layer of the cavity.

From Figure 21, it is noted that as the height of the cavity increases, the rate of heat transfer decreases. Figure 22 shows four plots: total energy, dissipation of kinetic energy, effect of magnetic field on velocity and changes in velocity each with respect to time from the time the fluid enters the cavity till when the fluid exits. It is evident that total energy within the cavity reduces with increase in time. Effect of magnetic field is strongly felt as the velocity reduced with time. However, the overall velocity increased with time. This is attributed to increase in Rayleigh number, which determines the domination of buoyant forces over viscous forces. Total rate of kinetic energy dissipation reduces with increase in time. It was computed from $\varepsilon = U_j \frac{\partial U_i}{\partial x_j} \frac{\partial U_j}{\partial x_i}$. From Figure 22, we note that energy reduces with time inside the cavity. This depends on the velocity, temperature and the Rayleigh number as it determines the temperature distribution and the velocity with which the fluid flows inside the cavity.

3.4 Validation of Results

Our results were compared with those of Ozoe *et al.* (1986) who considered Turbulent Natural Convection in a Cubical Enclosure heated from below, cooled on a portion of one vertical side wall and insulated on all other surfaces. A top view of the velocity vector revealed a downward spiral flow near the side walls along the cooled vertical wall. A weak spiral flow was also found along the side walls near the wall opposing the partially cooled one. These results show good agreement with this study. For the present study, the flow near the centre of the enclosure is less spiral as compared to that near the side walls as illustrated by all the figures on velocity profiles.

4.0 CONCLUSION

From the numerical simulations done in this study, it is noted that the velocity intensity at the core and near side walls was different and precisely at the core it was higher than near side walls. The results show that the transverse magnetic field has an important influence on the overall motion of the fluid and heat transfer within the room. It retards the velocity of the fluid within the enclosure and reduces the rate of heat transfer. Thus, magnetic field suppresses turbulence fluid flow.

Verosity, and temperature profile magnitudes and intensity

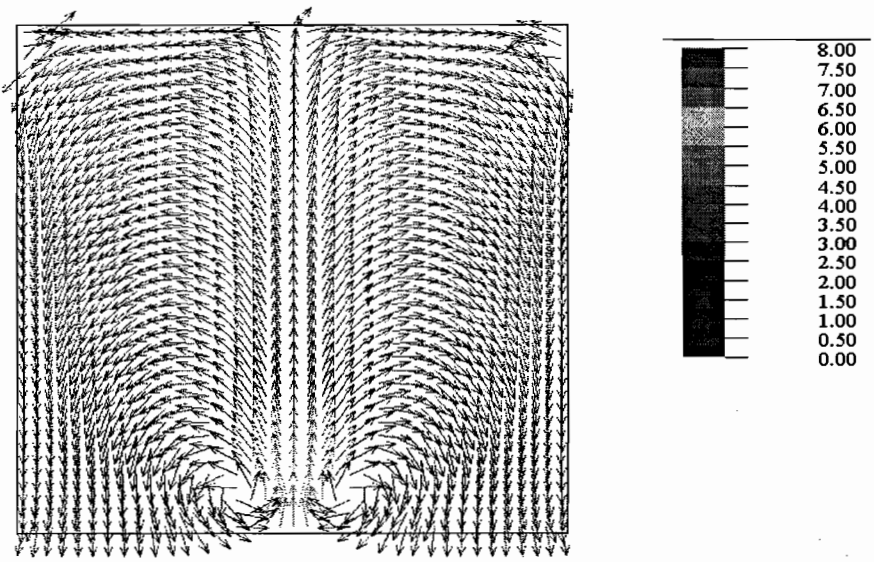

Figure 5: Velocity profiles at X=0.1, Ra =5x10^{11}, Ha=0

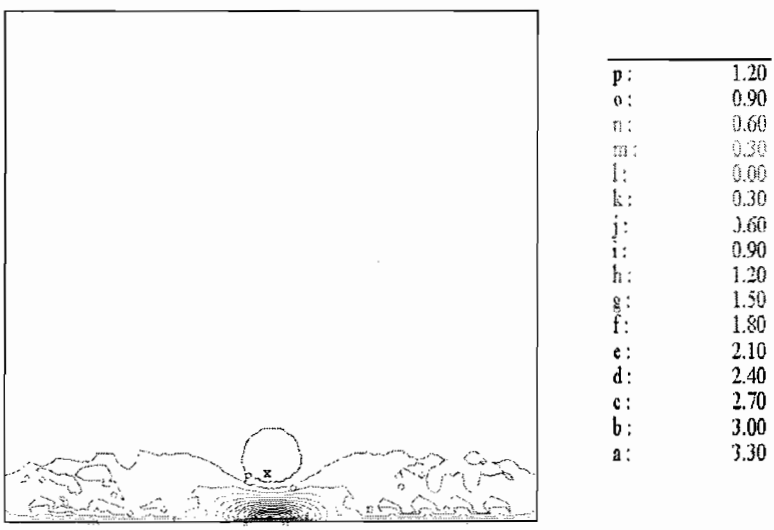

Figure 6: Temperature profiles at X=0.1, Ra=5x10^{11}, Ha=0

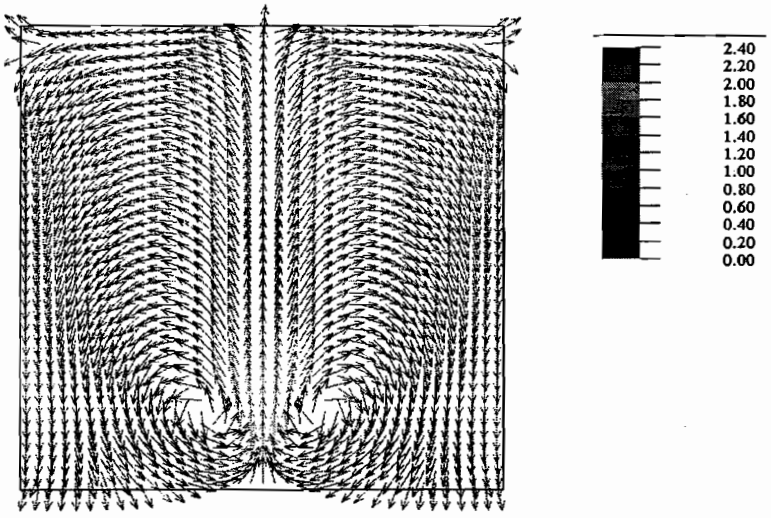

Figure 7: Velocity profiles at X=0.3, Ra =5x10^{12}, Ha=50

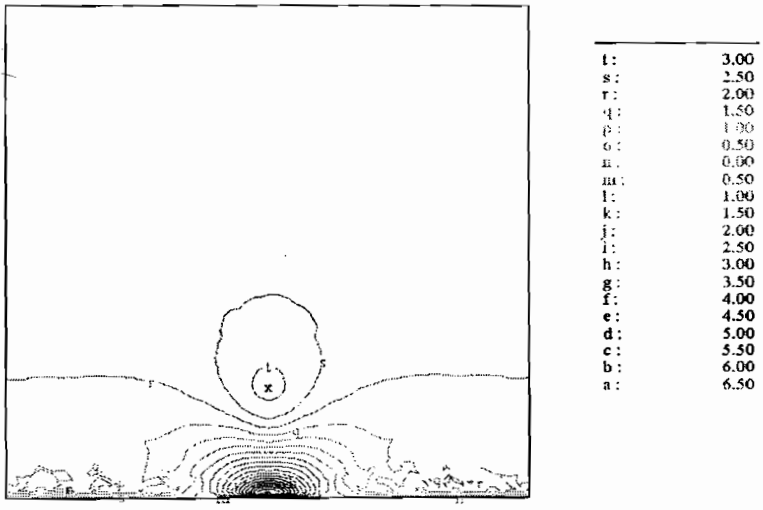

Figure 8: Temperature profiles at X=0.3, Ra=5x10^{12}, Ha=50

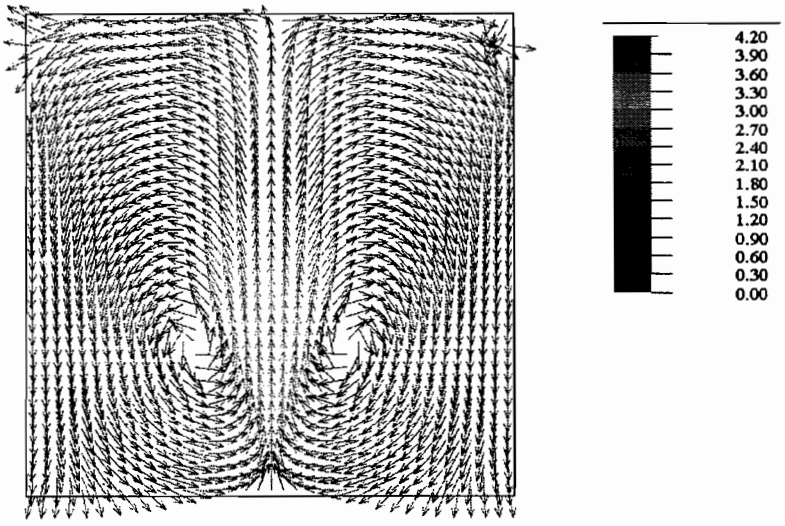

Figure 9: Velocity profiles at Y=0.1, Ra =5x10¹², Ha=50

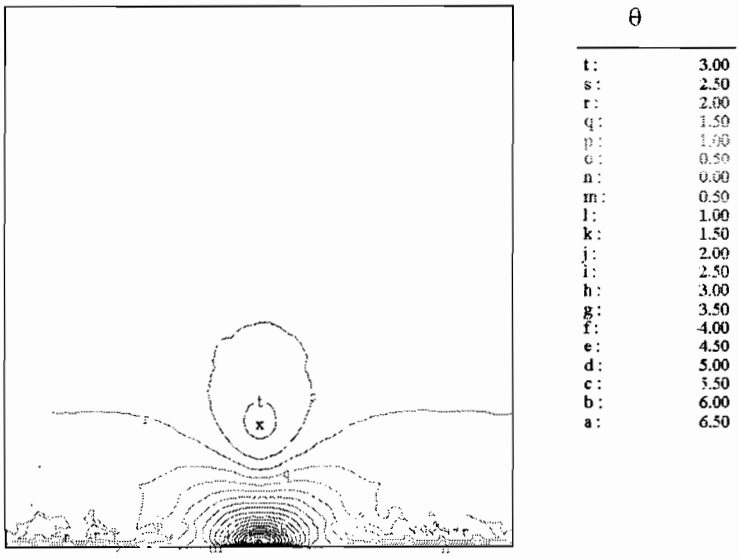

Figure 10: Temperature profiles at Y=0.1, Ra=5x10¹², Ha=50

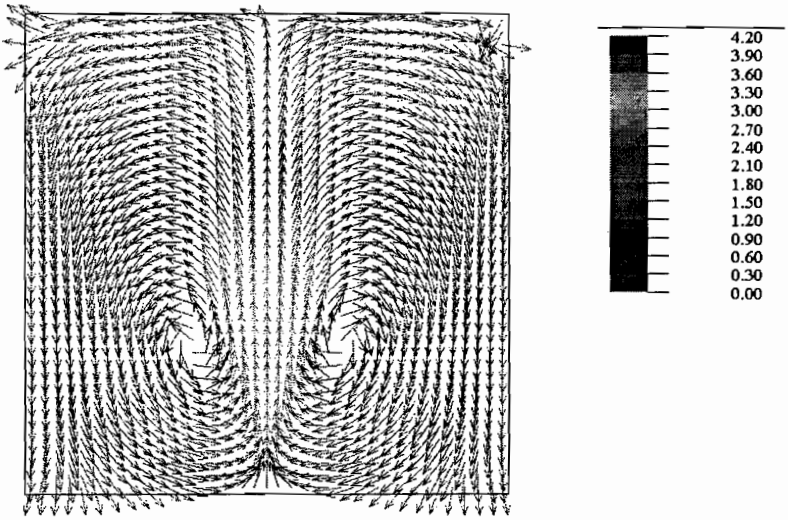

Figure 11: Velocity profiles at Y=0.3, Ra =5x10^{13}, Ha=50

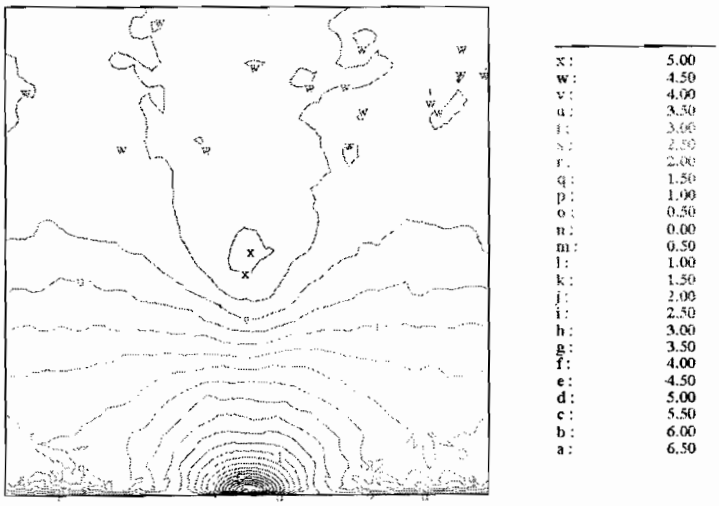

Figure 12: Temperature profiles at Y=0.3, Ra=5x10^{13}, Ha=50

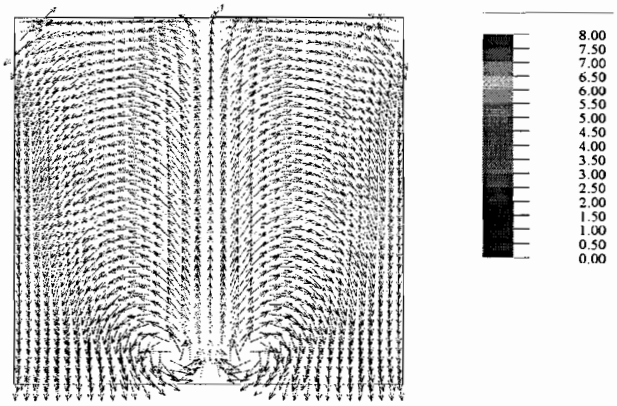

Figure 17: Velocity profiles at X=0.5, Ra =5x10^{12}, Ha=50

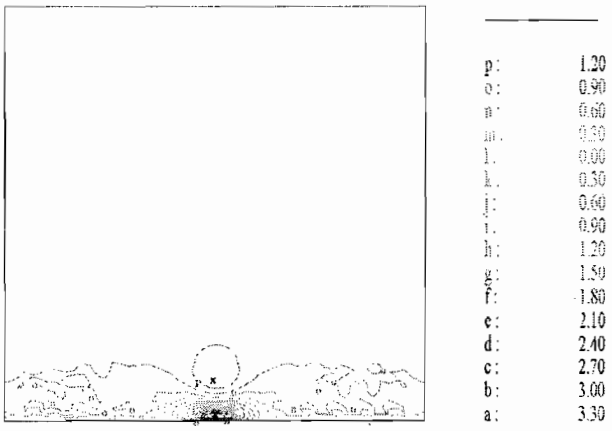

Figure 18: Temperature profiles at X=0.5, Ra=5x10^{12}, Ha=50

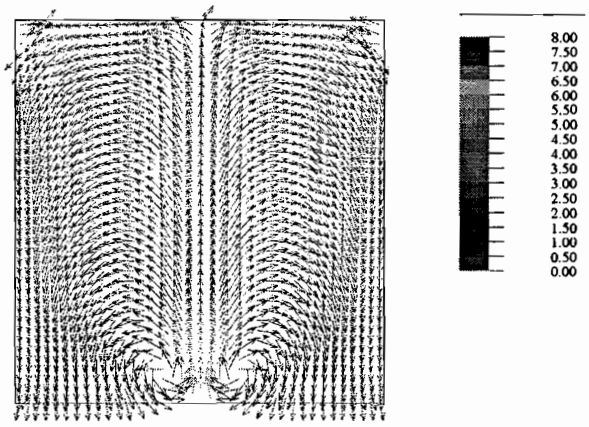

Figure 19: Velocity profiles at X=0.9, Ra =5x10^{12}, Ha=50

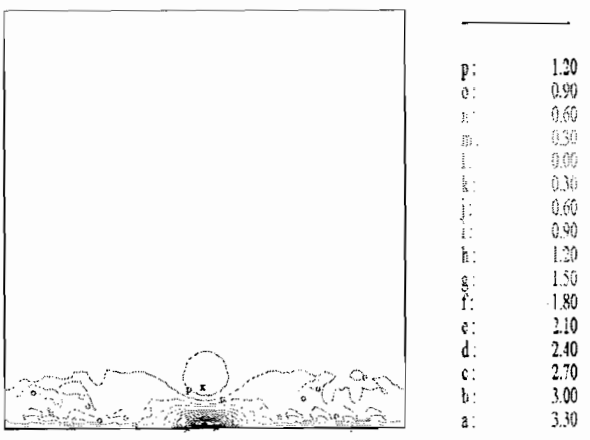

Figure 20: Temperature profiles at X=0.9, Ra=5x10^{12}, Ha=50

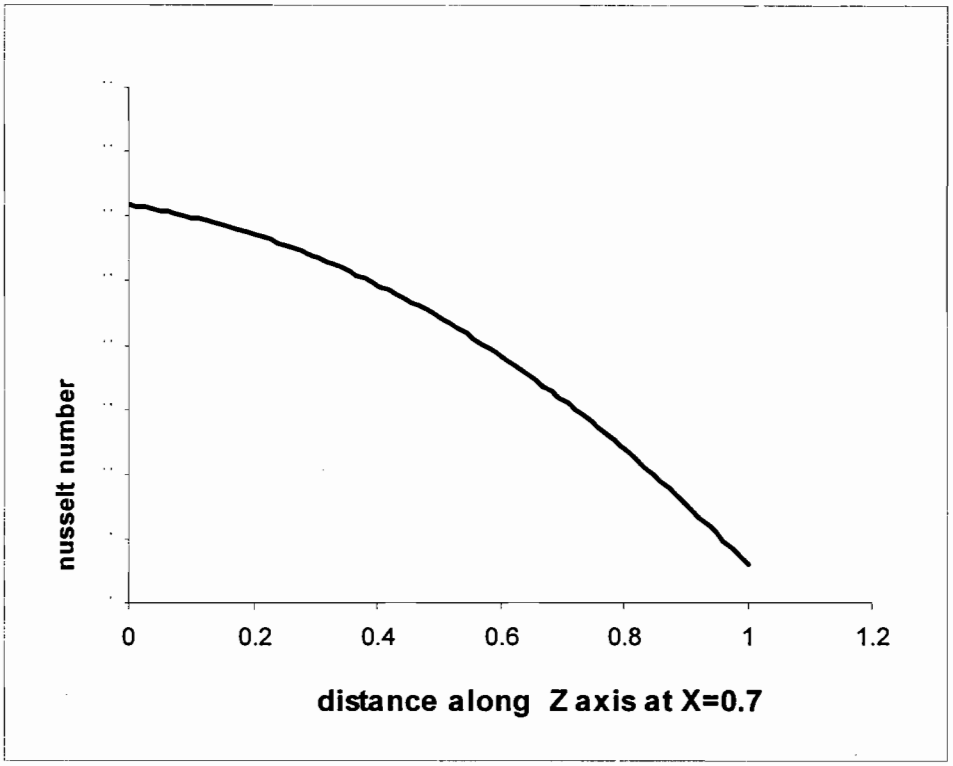

Figure 21: Variations of Nusselt number along the z-axis

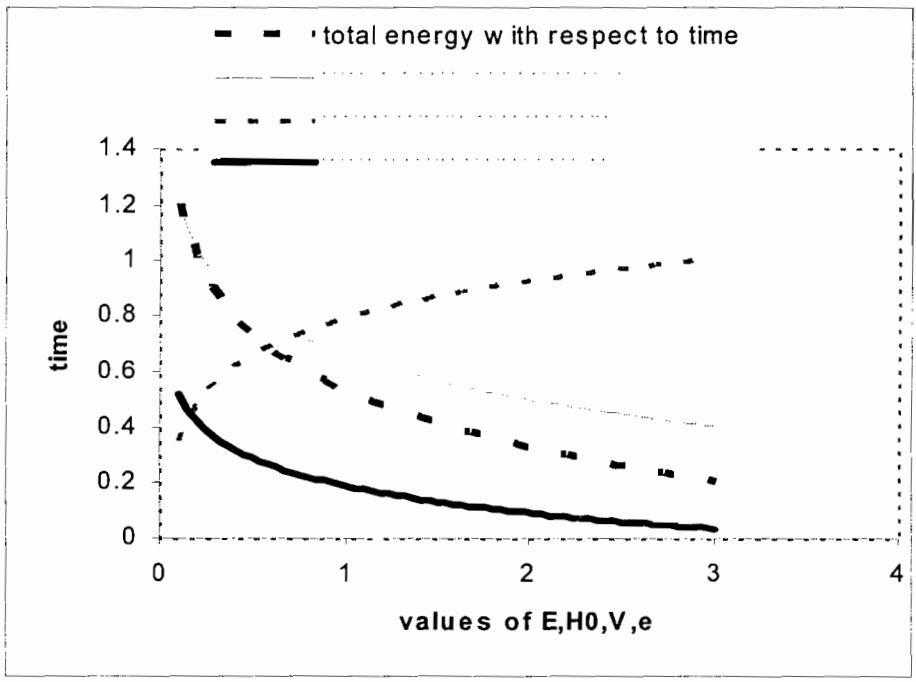

Figure 22: Plot on dissipation rate of turbulent kinetic energy (solid line), fluid velocity (dotted), total energy (long dash) and the effect of magnetic field on fluid velocity with respect to time

REFERENCES

Alboussiere T., Garandet J. P. and Moreau R. (1992). Buoyancy-driven Convection in a Rectangular Enclosure with a Transverse Magnetic Field, *Int. J. Heat and Mass Transfer*, **32**, pp 779-797.

Alboussiere T., Garandet J. P. and Moreau R. (1993). Effect of Slight Non-uniformity of the Magnetic field on MHD Convection, *Int. J. Heat and Mass Transfer*, **32**, pp 674-692.

Aleksandrova S. and Molokov S. (2000). Three-Dimensional Buoyant Convection in a Rectangular Cavity with Differentially Heated Walls in a Strong Magnetic Field. Proc. 3rd Int. Conference on Electromagnetic Processing of Materials Japan ISIJ, pp153-159.

Awbi H. B. (1989). Application of Computational Fluid Dynamics in Room Ventilation *Building and Environment*, **24**, pp 121-127.

Branover G. G., Kit L.G. and Platmiks J. A. (1993). Effects of Transverse Magnetic Field on the Intensity Profiles of Turbulent Velocity Distribution in a Channel of Rectangular Cross-section, International Association for Hydraulic Research, Delft, The Netherlands, **2**, pp 530-536

Daly B. J. and Harlow F. H. (1970). Transport Equations of Turbulence. *Physics of Fluids*, **7**, pp 2634-2649.

Faraday, M. (1839), Experimental Research in Electricity, Richard and John Edward Taylor.

Hague, S and Arajs, T. (1994). Convective Flows in Presence of Magnetic Field and Gravitational Force in an Enclosure. (Numerical and Experimental study) Univ. of Lagos, **15**, pp 216-221

Harlow F., Andre H., and Welch J.E. (1965), Numerical Calculation of Time-dependent Viscous Incompressible Flow of Fluid with Free surface. *The Physics of Fluids,* **8**, pp13.

Henry D., and Kaddeche S. (1993). Note on Stabilisation Laws of Numerical Methods used in Simulation of Computational Fluid Dynamic Problems for Heat Transfer in an Enclosure. *J. Heat Transfer*, **33**, pp 64-71.

Holman T. M. (1979), Numerica Simulation of High Rayleigh number Convection, *Journal of Science and Computing*, **4**, pp219-236.

Hoogendorn, C.J. (1986), Natural Convection in Enclosures, Proc. 8th Int. Heat Transfer conference. Tin *et al Ed. Hemisphere*, Washington.

Ince, B. E. and Launder (1985), On Computation of Convective Heat Transfer in Complex Turbulent flows. *Transaction of ASME,* **110**, pp1112-1128.

Lilley, D.G (1991), Three-Dimensional Flow Prediction for Industrial Mixing. ASME International Computers in Engineering Conference.

Ming L. and Tang T. (2001). A Compact Fourth-Order Finite Difference Scheme for Unsteady Viscous Incompressible Flows. *Int. Journal of Scientific Computing,* **25**, pp15-23.

Ozoe H. Mouri, A, Hiramitsu M. Churchill S.W. and Lior N. (1986). Numerical Calculation of the Three Dimensional Turbulent Natural Convection in Cubical Enclosure. *Journal of Heat Transfer,* **108**, pp 806-813.

Piomelli U.(1999), Large-Eddy Simulation; Achievements and Challenges. *Progress in Aerospace Science,* **35**, pp335-362.